Research Article **Phytopharmacology Research Journal (PRJ) Open Access**

Received: 5 November 2025 | Revised: 6 December 2025 | Accepted: 7 December 2025 | Published online : 15 December 2025 | ISSN : 2959-9687

PVA composite for drug delivery and electrochemical application

Dawood khan[1], Said Mubassir[2*], Shahid Ali[1], Ijaz ahmad[1], Ajmal Shah[3], Ali Khan[4*]

[1]Department of Chemistry, Abdul Wali Khan University, Mardan, Pakistan

[2]Department of Zoology, Abdul Wali Khan University, Mardan, Pakistan

[3]School of Chemistry, Xi'an Jiaotong University, China

[4]Chemistry Engineering Materials Environment Group (CEMEG), Faculty of Science and Engineering, Swansea University, Swansea SA1 8EN, UK

⁎Correspondence
SAID MUBASSIR
Saidmubassir@gmail.com

ALI KHAN
2445119@swansea.ac.uk

Funding information
This study is self-funded by the students. with no external support.

Abstract

PVA grafted polymer has been becoming a promising sustainable material for high function needs. In this work, a derived monomer was incorporated onto the PVA backbone successfully to create an environmentally friendly polymer system that can have relevance for drug delivery and electrochemical applications. The derived monomer's grafting with the PVA was confirmed using Fourier transform infrared spectroscopy analysis which showed the emergence of characteristic functional groups and variations in hydrogen bonding interactions. X-ray diffraction analysis showed great modifications in the crystalline structure of PVA after grafting (reduced crystalline and increased amorphous character due to the introduction of grafted chains). Thermogravimetric analysis revealed enhanced thermal stability of the grafted polymer as compared to pristine PVA and was attributed to the presence of PVA functional moieties as well as variations in polymer chain interactions. The structural, crystalline and thermal modifications in the grafted PVA indicate its potential use as a multifunctional polymer platform, where increase in amorphous nature and thermal stability is desired for controlled drug delivery systems and electrochemically active polymer matrices. This work provides evidence of the potential of grafted PVA as a sustainable material for biomedical (Drug delivery) and electrochemical applications in the future.

KEYWORDS

Graft polymerization, FTIR, XRD, TGA, Drug delivery, Electrochemical applications

1.0 INTRODUCTION

Poly(vinyl alcohol) (PVA) is a widely studied synthetic polymer because of its good film-forming ability, chemical resistance, hydrophilicity, non-toxicity and good biocompatibility, which are attractive attributes for biomedical, packaging and electrochemical applications. To overcome these limitations, chemical modification of PVA by grafting has been extensively used to tailor the structural and physicochemical properties of the PVA [1]. Graft copolymerization of functional vinyl monomers appears to be a good method to introduce functional groups onto the PVA backbone to vary the crystalline, the hydrophilicity, and the thermal behavior of the resulting polymers. Methacrylic acid (MAA), with the presence of reactive carboxylic acid groups, is often used in order to enhance the pH sensitivity, the intermolecular interactions and the compatibility with the active agents in polymeric systems [2]. Acrylonitrile (AN) is another important monomer used in grafted polymer systems because of the presence of nitrile groups that provide enhanced mechanical strength, chemical resistance and thermal stability. Incorporation of acrylonitrile segments into polymer matrices has been shown to minimize excessive swelling and enhance structural rigidity which is desirable for applications which require dimensional stability [3]. In recent years, polymer-nanoparticle composites have attracted much interest owing to the added multifunctional properties that are obtained through the synergistic combination of the polymer matrix and nanofillers. Among different types of metallic nanoparticles, silver nanoparticles (AgNPs) are of special interest because of their high thermal stability, electrical conductivity and high interactivity with polymer functional groups such as hydroxyl and carboxyl moieties. [4]. The AgNPs incorporation into the polymer systems based on PVA has been found to modify the crystalline structure and reduce mobility of the polymer chains and results in increased thermal resistance. In addition, AgNPs can also be used as effective fillers in the case of AgNPs in the composites to reduce the uptake of water and swelling due to the formation of physical interactions and coordination bonds with the polymer chains [5]. Silver nanoparticles (AgNPs) are particularly relevant because they provide high electrical conductivity, useful interfacial interactions with hydroxyl/carboxyl groups, and broad utility in biomedical and functional materials [6]. Natural can be modified for different applications [7]. Thermal stability is another key requirement for polymeric drug carriers and electrochemical membranes, and PVA-based systems often show multi-step mass loss in TGA related to moisture removal and subsequent backbone degradation [8]. Nanofillers frequently alter degradation pathways by restricting chain mobility and modifying heat/mass transfer, which can shift decomposition behavior and increase high-temperature residue compared to neat polymers [9]. Accordingly, this work focuses on a PVA-based grafted system containing methacrylic acid and acrylonitrile and evaluates the influence of graded AgNP loading on polymer–filler interactions, crystallinity, and thermal stability. Structural changes are examined by FTIR (functional group identification and interaction shifts), crystallinity and Ag phase confirmation are evaluated using XRD, and thermal decomposition behavior is assessed via TGA, alongside swelling behavior to link structure to aqueous performance [10].

Despite several reports on PVA-based graft copolymers and polymer–silver nanocomposites, systematic studies focusing on the combined effect of methacrylic acid, acrylonitrile, and varying concentrations of silver nanoparticles on the structural, crystalline, thermal, and swelling behavior of PVA-based systems remain limited. Therefore, the present work aims to develop and characterize PVA grafted with methacrylic acid and acrylonitrile and reinforced with different loadings of silver nanoparticles. The influence of AgNP concentration on functional group interactions, crystallinity, thermal stability, and swelling behavior is investigated using Fourier transform infrared spectroscopy (FTIR), X-ray diffraction (XRD), thermogravimetric analysis (TGA), and swelling studies.

2.0 Materials and Methods

Low molecular weight chitosan (Mw 50–190 kDa, degree of deacetylation ≈ 83%), sodium hydroxide (NaOH),

potassium persulfate (KPS), hydrochloric acid (HCl), acrylic acid (AA), 2-acrylamido-2-methylpropane sulfonic acid (AMPS), acrylonitrile (AN), and *N,N′*-methylenebisacrylamide (MBA) used as a crosslinking agent were purchased from Sigma-Aldrich (Schnelldorf, Germany) and used without further purification. Poly (vinyl alcohol) (PVA) was employed as the polymer backbone material. Silver nanoparticles (AgNPs) were incorporated as the inorganic nanofiller.

2.1 Instrumentations

Fourier transform infrared (FTIR) spectra were recorded using a Nicolet iS5 spectrometer (Thermo Scientific, Germany). The surface morphology of the samples was examined using a scanning electron microscope (SEM) (JEOL JSM-5910, Tokyo, Japan). Thermogravimetric analysis (TGA) was carried out using a PerkinElmer thermogravimetric analyzer (Singapore). X-ray diffraction (XRD) measurements were taken with a D-2 Phaser diffractometer (Bruker, Karlsruhe, Germany) to analyze the crystalline structure of the prepared samples.

2.2 Preparation of PVA-Based Composite Samples

An aqueous solution of poly (vinyl alcohol) (PVA) was first prepared by dissolving a predetermined amount of PVA in deionized water under continuous stirring at 80–90 °C until a clear and homogeneous solution was obtained. After full dissolving, the solution was cooled down to room temperature. Methacrylic acid (MAA) and acrylonitrile (AN) were then added to a PVA solution in constant stirring condition to obtain a uniform mixing. Potassium persulfate (KPS) was introduced as an initiator of free radical polymerisation followed by N,N'-methylenebisacrylamide (MBA) as a cross-linking agent. The reaction mixture was kept under constant stirring, so to allow the graft copolymerization reaction to proceed, forming PVA/MAA/AN composite, which has been called Sample 1.

For the preparation of silver nanoparticle reinforced composites similar procedure was followed with the incorporation of silver nanoparticles at different concentrations. Specifically, 0.1 g, 0.2 g and 0.3 g of silver nanoparticles were already dispersed in deionized water separately by magnetic stirring (and/or ultrasonication if applicable) to achieve uniform dispersion. These dispersions were then added dropwise to the PVA/MAA/AN reaction mixture before the initiation of grafting to get Sample 2, Sample 3, and Sample 4, respectively. The resulting mixtures were stirred continually to obtain homogeneous distribution of Ag nanoparticles in the polymer matrix. After completion of the reaction the composites were cooled to room temperature, washed thoroughly with deionized water to remove unreacted monomers and residual reagents and finally dried at ambient temperature (or in a vacuum oven) to constant weight.

2.3 Swelling study

The swelling behavior of the prepared PVA-based composite samples was investigated by immersing 0.1 g of each dried sample in 100 mL of distilled water at room temperature for a period of 24 h. After the swelling period, the samples were removed from the solution, gently blotted with filter paper to eliminate excess surface water, and weighed immediately. The degree of swelling was quantitatively determined using Eq. (1).

$$\text{Swelling ratio (\%)} = \frac{(M_2 - M_1)}{M_1} \times 100 \qquad (1)$$

where M_1represents the initial dry mass of the composite sample (in grams) before immersion in distilled water, and M_2represents the final wet mass of the sample (in grams) after completion of the swelling process.

3.0 RESULTS AND DISCUSSION

3.1 FTIR analysis

The FTIR spectra of all samples proved the successful formation of PVA-methacrylic acid-acrylonitrile polymer system, and the interaction of silver nanoparticles with polymer matrix. A broad absorption band in the region of 3200-3600 cm-1 is due to O-H stretching vibration of PVA and is indicative of large amount of hydrogen bonding present in the polymer network [11]. The presence of methacrylic acid has been confirmed by the presence of the strong carbonyl (C=O) stretching band around 1700-1725 cm-1 [2]. While the absorption peak at around 2240-2250 cm-1 is the characteristic sharp absorption feature, which is attributed to the nitrile (C[?]N) stretching vibration of the acrylonitrile units. Additional bands found at around 2920-2950 cm-1 as well as 1080-1140 cm-1 are attributed to C-H stretching and C-O stretching vibrations of the PVA backbone, respectively [3]. Upon incorporation of silver nanoparticles (Samples 2 to 4) slight broadening and small shifts of the O-H and C=O bands are registered, suggesting coordination interactions between Ag nanoparticles and hydroxyl/carboxyl functional groups of the polymer matrix [12]. These spectral changes are more profound as the Ag content increases and is indicative of the good interaction and dispersion of the Ag nanoparticles in the polymer system.

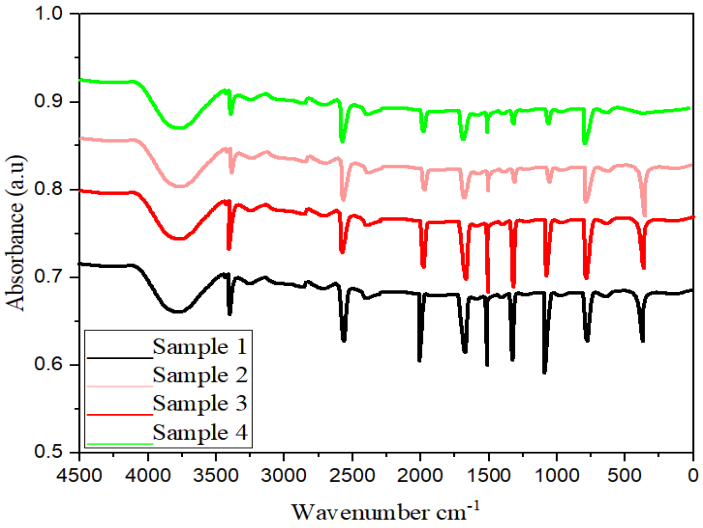

Fig. 1. FT-IR analysis of sample 1, sample 2, sample 3, and sample 4

3.2 XRD Analysis

X-ray diffraction analysis is used to gain some insight into the crystalline structure of the polymer matrix as well as verifying the incorporation of silver nanoparticles. Sample 1 (without Ag nanoparticles) shows a wide-diffraction peak of 2 theta 19~20deg, typical of the semi-crystalline nature of PVA [13]. The wide extent of this peak indicates the low crystalline caused by the presence of methacrylic acid and acrylonitrile segments, which break up the regular packing of the chains of PVA. With the addition of silver nanoparticle (Samples 2 to 4), distinct diffraction peaks are obtained at about 38.1, 44.3, 64.4, and 77.5 [14], corresponding to the (111), (200), (220) and (311) crystallographic planes of the face-centered cubic (fcc) metallic silver. The intensity of these peaks, associated with Ag, increases with the Ag nanoparticle content in the case of successful incorporation and crystalline nature of silver in the polymer matrix [15]. Simultaneously the crystalline peak of the PVA is showing a progressive decrease of intensity, suggesting that Ag nanoparticles further impede the ordering of the polymer chains and

increase amorphous nature of the system [16].

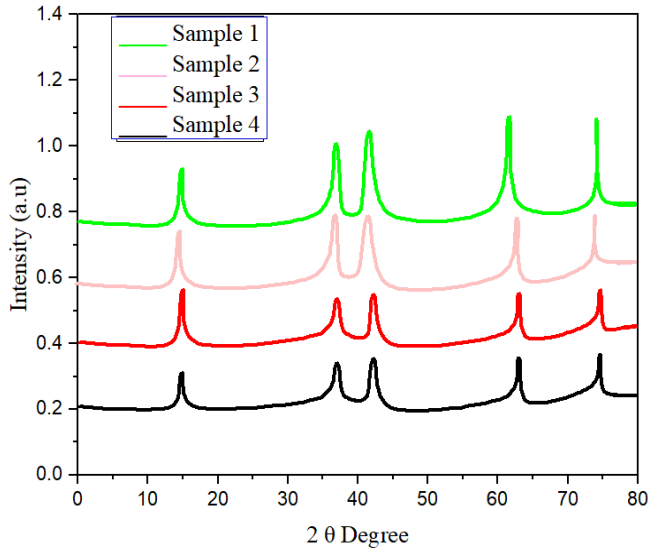

Fig. 2. XRD analysis of sample 1, sample 2, sample 3, and sample 4

3.3 TGA Analysis

Thermogravimetric analysis was used to study the thermal stability of the prepared polymer composites. The multi-step degradation pattern is observed for all the samples. The initial loss of weight below about 120deg is caused by evaporation of physically adsorbed/bound moisture [17], which is typical for PVA-based systems because of their hydrophilic nature; The second degradation step occurring in the range of approximately 200-320 degC is related to both decomposition of the side groups of methacrylic acid and dehydration reactions of the polymer chains [18]. The major weight loss that is observed is between 350 and 500degC can be attributed to the thermal breakdown of the main polymer backbone. With higher concentrations of silver nanoparticles (Samples 2-4), the onset of degradation is slightly shifted towards higher values which is an attribute of enhanced thermal stability [5]. Additionally, the amount of residual mass at higher temperatures increases with Ag loading, which is attributed to the presence of thermally stable metallic silver as well as increased char formation [4]. These results show that the addition of Ag nanoparticles leads to the enhancement of thermal resistance of the polymer system based on PVA.

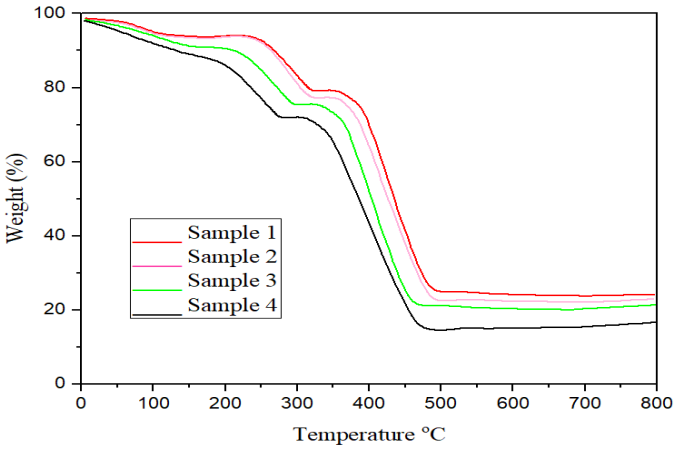

Fig. 3. TGA analysis of sample 1, sample 2, sample 3, and sample 4

3.4 Swelling Ratio

The swelling behavior of the prepared PVA based composites is strongly influenced by the grafted polymer network structure and silver nanoparticles. As seen from the swelling ratio results, Sample 1 (PVA /MAA /AN without Ag nanoparticles) has the highest swelling ratio that can be explained by the hydrophilic nature of PVA and the presence of carboxylic acid from methacrylic that absorbs water through hydrogen bonding interactions. Similar behavior in swelling has been widely reported for PVA-based grafted and hydrogel systems owing to their high affinity for water molecules [1]. With incorporation of silver nanoparticles in Samples 2 to 4 gradual decrease in the ratio of swelling is obtained with the increase in the amount of silver. This reduction in the swelling can be ascribed to restriction in polymer chain mobility due to interaction between the Ag nanoparticles and the functional groups such as hydroxyl (-OH) and carboxyl (-

COOH) groups present in the polymer matrix. These interactions behave as additional physical points of cross-linking and therefore limit the penetration of water into the polymer network [5]. Furthermore, the presence of acrylonitrile segments plays an important role in the decreased swelling behavior due to the increase in the rigidity and hydrophobic character of the polymer network. Nitrile-containing polymer chains are known to reduce water uptake and enhance dimensional stability and so the lower swelling ratios observed in the Ag-reinforced samples [3]. The lowest swelling ratio recorded for Sample 4, having the highest amount of Ag nanoparticles indicated the formation of a more compact and dense structure of polymer formations. Higher nanoparticles loading improves filler-polymer interactions and minimizes free volume in the network and hence limits diffusion of water into the composite. Similar trends of reduction in swelling with increasing content of inorganic filler have been reported for several polymer nanocomposite systems [4].

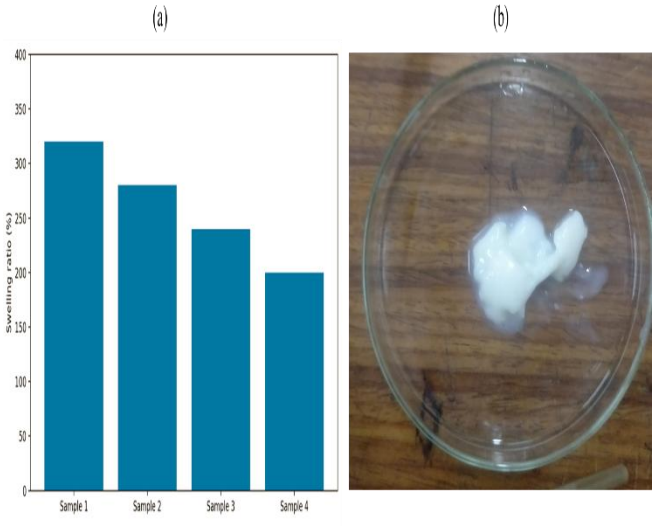

Fig. 4 (a). Swelling ratio of sample 1, sample 2, sample 3, and sample 4 and 4 (b) swell sample 4

3.5 Electrochemical Performance Analysis

The electrochemical behavior of the prepared PVA-based composites was tested by cyclic voltammetry (CV) and galvanostatic charge-discharge (GCD) measurements as shown in Fig. 5 (a-d). Figures 5 (a) and (b) give the CV curves measured at various scan rates, and Figs. 5 (c) and (d) give the corresponding GCD profiles at a variety of current densities.

3.5.1 Cyclic Voltammetry and Galvanostatic Charge Discharge Analysis

As can be seen in Fig. (a) and Fig. (b) the CV curves have quasi-rectangular shapes with small redox humps, which is related to the combination of electric double-layer capacitance (EDLC) behavior and pseudocapacitive contributions due to redox-active functional groups and metal-polymer interactions. The increase in current response with increasing scan rate (10-100 mV s-1) is suggestive of good electrochemical reversibility and rapid charge transport within the electrode material. Such behavior is typical for polymer-based composites with conductive fillers or metal nanoparticles, as a result of enhanced ion diffusion occurring and electron transfer at electrode-electrolyte interface [19]. Furthermore, the maintenance of CV shape at increased scan rates is indicative of good rate capability and structural stability of the composite material. The presence of silver nanoparticles is responsible for better electrical conductivity because of the formation of conductive pathways in the polymer matrix, which is responsible for faster electron transport. Similar improvements in current response from Ag nanoparticles incorporation has been reported in polymer based electrochemical systems [20]. The GCD curves in Fig. (c) and Fig. (d) exhibit almost symmetrical triangular profiles as functions of different current densities (0.5-4 A g-1), which confirms good

capacitive behavior as well as high coulombic efficiency. The linear relationship between voltage and time of both the charging as well as discharging process implies efficient energy storage and low internal resistance. Deviations from the perfect linearity may be attributed to faradaic redox reactions involved in metal-polymer and functional groups interactions [21]. As the current density increases, it affects the discharge time which is quite common in supercapacitor type materials because of the low ion diffusion at high current loads. However, the composites still have appreciable discharge time even at higher current density, which shows good rate performance. The longer discharge duration found for samples containing Ag suggests that the discharge capability is increased, and this can be explained by the synergy of polymer matrix and silver nanoparticles [22]. The improved electrochemical performance can be interpreted by synergy from the grafted polymer network, which is based on PVA, and the inserted Ag nanoparticles. The polymer matrix is responsible for mechanical integrity and ion-accessible pathways, and Ag nanoparticles are responsible for electronic conductivity and interfacial charge transfer. This synergistic interaction is responsible for reducing internal resistance and enhancing electrochemical kinetics to provide higher current response and better charge discharge behavior [23]. Overall, both CV and GCD confirm that the prepared PVA-based composites possess good electrochemical behavior, such as high reversibility, high rate capability and stable process on charge and discharge. These features make the materials suitable candidates for electrochemical energy storage and so on. [24].

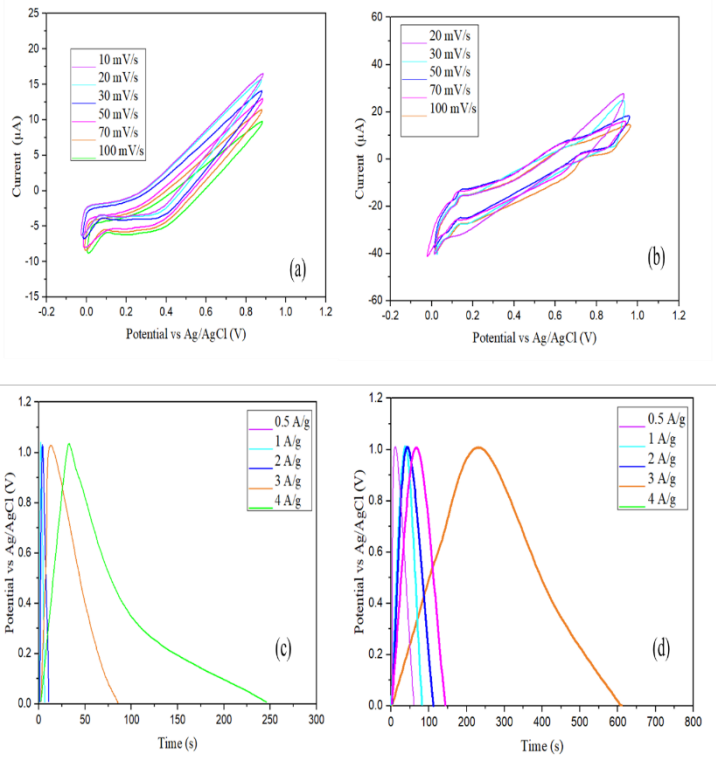

Fig. 5. Electrical properties analysis for sample 1, and sample 4

3.6 Loading and Release study

The effect of pH on ibuprofen adsorption onto Sample 1, Sample 2, Sample 3, and Sample 4 was investigated over a pH range of 2–12, as shown in the figure 6. For all samples, the adsorption capacity increased with increasing pH and reached a maximum at pH 4, followed by a gradual decrease at higher pH values. At pH 4, the maximum adsorption capacities were approximately 97 mg g^{-1} for Sample 1, 103 mg g^{-1} for Sample 2, 117 mg g^{-1} for Sample 3, and 130 mg g^{-1} for Sample 4. The enhanced adsorption at pH 4 can be attributed to favorable interactions between ibuprofen molecules and the functional groups present in the composites. At higher pH values, reduced adsorption is observed due to increased ionization of ibuprofen, leading to electrostatic repulsion with negatively charged sites on the composite surface [25].

The effect of contact time on adsorption of ibuprofen over Sample 1, Sample 2, Sample 3 and Sample 4 was investigated for a contact time duration of 20-240 min as given in figure 6. For all samples, fast adsorption capacity in the first stage can be observed during the first stage, which means fast diffusion of ibuprofen molecules towards the available active sites on the composite surface. A long-term plateau of the adsorption rate was reached after a time of around 120 min indicating the adsorption equilibrium is achieved. The highest adsorption capacities were around 79 mg g-1, 90 mg g-1, 110 mg g-1 and 120 mg g-1 for Sample 1, 2, 3 and 4 respectively. Platitude behavior in case of higher contact time can be explained by saturation of active adsorption sites and lower mass transfer. Consistent with the pH and the concentration studies, Sample 4 showed the greatest adsorption capacity followed by Sample 3, Sample 2 and Sample 1 [26].

The in vitro release behavior of ibuprofen from Sample 1, Sample 2, Sample 3 and Sample 4 was explored in phosphate buffered saline (PBS) in pH 7.4 as illustrated in figure 6. All samples showed a quick release in the early stage which can be explained by desorption of ibuprofen molecules which are loosely bound on the composite surface. This was followed by a slower and more sustained release phase which indicated diffusion-controlled transport of ibuprofen from the composite matrix. The cumulative release gradually increased with time and was found to be maximum around 88%, 82%, 79% and 75% for Sample 1, 2, 3 and 4, respectively after 240 min. Among the composites, Sample 1 showed the highest rate of drug release whereas Sample 4 showed the lowest release behavior, indicating more force persistence of interactions between drug and polymer in Sample 4 and the formation of a more compact chain structure. The Sustained Release Profile at Physiological pH (7.4) indicates the potential for these composites to be used for Controlled Drug Delivery applications [27].

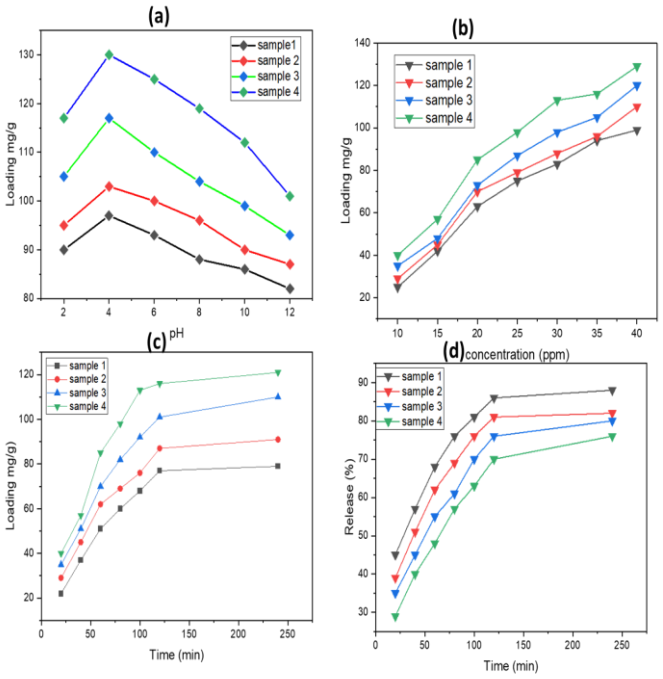

Fig. 6. Drug loading and release study using the as-prepared sample 1, sample 2, sample 3, and sample 4.

1.6.1 Freundlich isotherm model (FIM)

In 1906 Freundlich proposed Freundlich isotherm model (FIM) to describe adsorption on heterogeneous surfaces where adsorption is in multilayers and there are possible intermolecular interactions. According to this model, adsorption sites have different energies and as the surface coverage increases the adsorption energy decreases exponentially, making the process reversible. The Freundlich isotherm is linear & non-linear form and is given in Eq. (2), where Kf is the Freundlich adsorption capacity constant, while 1/n describes the adsorption intensity and surface heterogeneity.

$$\log qe = \log Kf + 1/n \log Ce \quad (2)$$

The Freundlich isotherm model was applied to evaluate the adsorption behavior of ibuprofen onto Sample 1, Sample 2, Sample 3, and Sample 4, and the corresponding parameters (Kf, n, and R^2) were determined through theoretical calculations. However, comparison of the experimental data with the fitted Freundlich model revealed a poor agreement, as reflected by relatively low correlation coefficients (R^2 = 0.864, 0.808, 0.767, and 0.755 for Sample 1, Sample 2, Sample 3, and Sample 4, respectively). These results indicate that the Freundlich model does not adequately describe the adsorption behavior of ibuprofen on the studied composites. The Freundlich isotherm plots for all samples are presented in **Fig**. 7 [28].

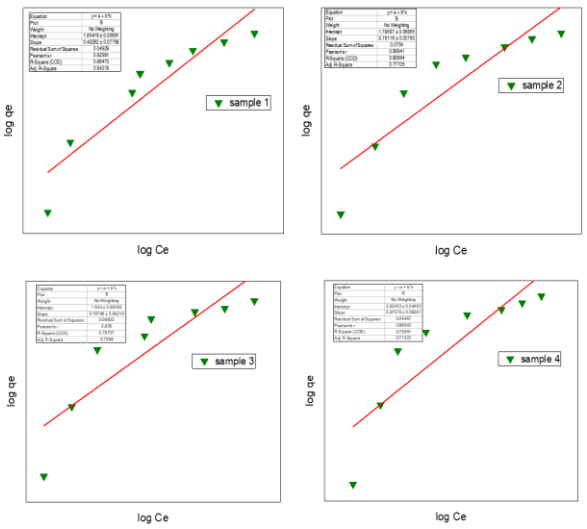

Fig. 7. FIM plots for the obtained data of adsorption of Ibuprofen on sample 1, sample 2, sample 3, and sample 4.

3.6.2 Langmuir isotherm model (LIM)

The Langmuir isotherm model (LIM), proposed by Irving Langmuir in 1913, describes adsorption as a monolayer process occurring on a homogeneous surface possessing a finite number of identical and energetically equivalent active sites. The model assumes that once a site is occupied, no further adsorption can occur at that site and that no interactions exist between adsorbed molecules on adjacent sites. The Langmuir isotherm can be expressed in both linear and non-linear forms. In the model equation, Qmax (mg g^{-1}) represents the maximum adsorption capacity corresponding to complete monolayer coverage of ibuprofen on the composite surface, KL denotes the Langmuir constant related to the adsorption energy, and Ce represents the equilibrium concentration of ibuprofen in solution. The Langmuir parameters (Qmax, KL, and R^2) were determined from the linear plots of 1/Ce, 1/q, as presented in Fig. 8.

$$Ce/qe = 1/ Qmax\ KL1+ Ce/Qmax \qquad (3)$$

The experimental data showed a good agreement with the Langmuir isotherm model for all composites, as evidenced by the high correlation coefficients (R^2 = 0.929, 0.947, 0.905, and 0.962 for Sample 1, Sample 2, Sample 3, and Sample 4, respectively). Furthermore, the calculated Qmax values were closely consistent with the experimentally obtained maximum adsorption capacities, confirming the validity of the Langmuir model. These results show that ibuprofen adsorption onto Sample 1-4 mainly takes place by a process of monolayer covering on a limited number of active sites. The good fitting to the Langmuir model indicates that the involvement of chemisorption that involves specific interactions between ibuprofen molecules and the functional groups present on the composite surface is dominating the adsorption mechanism [29].

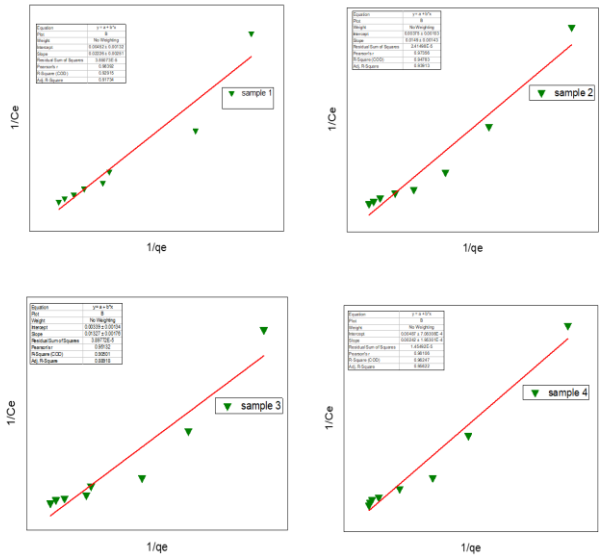

Fig. 8. LIM plots for the obtained data of adsorption of Ibuprofen on sample 1, sample 2, sample 3, and sample 4.

3.6.3 Pseudo first order kinetic model

Understanding the mechanism and pathways of the adsorption processes is important to interpret kinetics of drug carrier interaction. Among the different types of kinetic models, Lagergren kinetic model usually called pseudo-first order (PFO) kinetic model, which was proposed by Lagergren in 1898, is widely used to describe adsorption systems. The linear form of the PFO Kinetic equation (Eq. 4) in which K1 is the rate constant, q[?] is the adsorption capacity at equilibrium and q[?] is the adsorption capacity at any time, where is the contact time. To test the applicability of the PFO model experimental data were fitted by plotting t vs. ln(qe-qt).

$$\ln(qe-qt)=\ln qe-k1t \qquad (4)$$

Using this approach, the theoretical kinetic parameters were calculated for Sample 1, Sample 2, Sample 3 and Sample 4 using pseudo first order kinetic model. The correlation coefficients (R2) derived from the linear regression plots were 0.877, 0.807, 0.962 and 0.974 for Sample 1, Sample 2, Sample 3 and Sample 4 respectively. Although the R2 values varied from moderate to high for some of the samples, there were significant deviations between the experimental observed data and the theoretical predictions for the adsorption, implying that the kinetic model of PFO is unsatisfactory to describe the adsorption behavior of the system. These results suggest that the adsorption process is not only controlled by the first order of kinetics and other mechanisms may have a more dominant role in controlling the adsorption process [30].

3.6.4 Pseudo second order kinetic model

The Ho kinetic model or pseudo-second order (PSO) kinetic model was introduced by Ho and McKay in 1998 and is widely used to describe adsorption processes that are chemisorption-dominated. The linear form of the PSO kinetic model is expressed in Eq. (5), where K_2 represents the rate constant of the PSO model. The kinetic parameters were evaluated by plotting t/q_t versus t, and the corresponding linear fits are illustrated in Fig. 12.

$$t/q_t = 1/(k_2 q_e^2) + t/q_e \qquad (5)$$

The PSO kinetic model demonstrated a superior fit to the experimental data compared to the pseudo-first-order model for Sample 1, Sample 2, Sample 3, and Sample 4. The high correlation coefficients (R^2 = 0.975, 0.949, 0.970, and 0.930, respectively) confirm the strong agreement between the experimental data and the PSO model. The close correspondence between the calculated and experimental adsorption capacities further supports the suitability of the PSO model in describing the adsorption behavior. These results indicate that the adsorption process is controlled by the rate-determining step (RDS) associated with chemical interactions. Consequently, the adsorption of ibuprofen onto Sample 1–4 is predominantly governed by chemisorption mechanisms, involving strong

interactions between ibuprofen molecules and the active functional groups present on the composite surfaces [30].

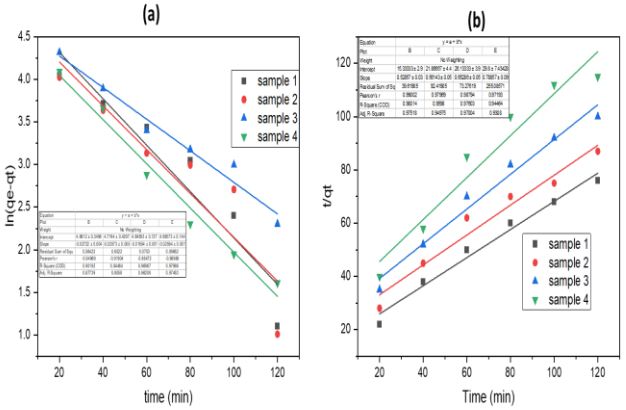

Fig: 9. Plots for the releasing of Ibuprofen on sample 1, sample 2, sample 3, and sample 4 representing the zero order and Higuchi model.

4.0 CONCLUSION

In this work, a sustainable PVA-based grafted polymer was successfully prepared by incorporation of a derived monomer on PVA backbone to produce an environmentally friendly polymer with superior functional qualities. Spectroscopic analysis showed successful grafting by occurrence of new characteristic functional groups and changes of hydrogen-bonding interactions. Structural analysis shows a serious reduction of crystallinity and an increment of the amorphous phase: this is due to the breaking of the packing of the PVA chains by the grafted segments. Thermal analysis showed the enhanced thermal stability of the grafted polymer as compared to the pristine PVA owing to the strong intermolecular interactions in the grafted polymer and its strengthened structures. The compatibility of structural, crystalline and thermal modifications elucidates the versatility of the grafted PVA system as a multifunctional polymer system platform. The resulting higher amorphous nature and thermal stability is especially beneficial from a controlled drug delivery system and electrochemically active polymer matrices perspectives. Overall, this work offers very solid evidence for the value of derived, grafted PVA polymers as a promising and sustainable alternative material to petroleum-derived materials for future biomedical and electrochemical applications.

ACKNOWLEDGMENTS

We thank all the students for their contributions and self-funding, as well as for their support**.**

CONFLICT OF INTEREST

The authors declare that they have no known competing financial interests or personal relationships that could have appeared to influence the work reported in this paper.

REFERENCES

1. Navarro, D.A., et al., *Xylogalactans from Lithothamnion heterocladum, a crustose member of the Corallinales (Rhodophyta).* Carbohydrate Polymers, 2011. **84**(3): p. 944-951.
2. Hsu, Y.-Y., et al., *Dendrons with urea/malonamide linkages for gate insulators of n-channel organic thin film transistors.* Reactive and Functional Polymers, 2016. **108**: p. 86-93.
3. Schappacher, M. and A. Deffieux, *Encapsulation of metallo-porphyrins into water-soluble amphipatic dendrigrafts.* Polymer, 2004. **45**(14): p. 4633-4639.
4. Tan, Z.H., et al., *Dynamic response of symmetrical and asymmetrical sandwich plates with shear thickening fluid core subjected to penetration loading.* Materials & Design, 2016. **94**: p. 105-110.
5. Gao, J., et al., *Electrically conductive polymer nanofiber composite with an ultralow percolation*

threshold for chemical vapour sensing. Composites Science and Technology, 2018. **161**: p. 135-142.
6. Yang, Y., et al., *A facile method for the fabrication of silver nanoparticles surface decorated polyvinyl alcohol electrospun nanofibers and controllable antibacterial activities.* Polymers, 2020. **12**(11): p. 2486.
7. Shah, M., et al., *Microwave-assisted synthesis of superabsorbent agar-based magnetic composite hydrogel for drug delivery and anti-inflammatory studies.* Results in Engineering, 2025. **26**: p. 104552.
8. Holland, B.J. and J.N. Hay, *The thermal degradation of poly(vinyl alcohol).* Polymer, 2001. **42**(16): p. 6775-6783.
9. Peng, Z. and L.X. Kong, *A thermal degradation mechanism of polyvinyl alcohol/silica nanocomposites.* Polymer Degradation and Stability, 2007. **92**(6): p. 1061-1071.
10. Minhas, M.U., et al., *Synthesis of chemically cross-linked polyvinyl alcohol-co-poly (methacrylic acid) hydrogels by copolymerization; a potential graft-polymeric carrier for oral delivery of 5-fluorouracil.* DARU Journal of Pharmaceutical Sciences, 2013. **21**(1): p. 44.
11. Mansur, H.S., et al., *FTIR spectroscopy characterization of poly (vinyl alcohol) hydrogel with different hydrolysis degree and chemically crosslinked with glutaraldehyde.* Materials Science and Engineering: C, 2008. **28**(4): p. 539-548.
12. Wang, F., et al., *Rapid synthesis of porous manganese cobalt sulfide grown on Ni foam by microwave method for high performance supercapacitors.* Synthetic Metals, 2019. **256**: p. 116113.
13. Morlin, B. and T. Czigany, *Cylinder test: Development of a new microbond method.* Polymer Testing, 2012. **31**(1): p. 164-170.
14. Talpur, M.Y., et al., *A simplified FTIR chemometric method for simultaneous determination of four oxidation parameters of frying canola oil.* Spectrochimica Acta Part A: Molecular and Biomolecular Spectroscopy, 2015. **149**: p. 656-661.
15. Khan, S., et al., *Lattice parameter instabilities during multi-phase precipitation in Alloy 693.* Journal of Alloys and Compounds, 2017. **700**: p. 149-154.
16. Cheng, X., et al., *The influence of mould pre-heat temperature and casting size on the interaction between a Ti–46Al–8Nb–1B alloy and the mould comprising an Al2O3 face coat.* Materials Chemistry and Physics, 2014. **146**(3): p. 295-302.
17. Wang, P.-P., et al., *Thermochemistry of two lead borates; Pb(BO2)2·H2O and PbB4O7·4H2O.* Thermochimica Acta, 2011. **512**(1): p. 124-128.
18. Gómez-Elvira, J.M., R. Benavente, and M.C. Martínez, *Unravelling the contribution of chain microstructure in the mechanism of the syndiotactic polypropylene pyrolysis.* Polymer Degradation and Stability, 2013. **98**(6): p. 1150-1163.
19. Nath, A.K. and A. Kumar, *Scaling of AC conductivity, electrochemical and thermal properties of ionic liquid based polymer nanocomposite electrolytes.* Electrochimica Acta, 2014. **129**: p. 177-186.
20. Li, C., H. Yi, and D. Lee, *On-demand supply of slurry fuels to a porous anode of a direct carbon fuel cell: Attempts to increase fuel-anode contact and realize long-term operation.* Journal of Power Sources, 2016. **309**: p. 99-107.
21. Wang, D., et al., *Structural hybridization of ternary (0D, 1D and 2D) composites as anodes for high-performance Li-ion batteries.* Energy Storage Materials, 2018. **13**: p. 293-302.
22. Chen, X., et al., *A self-powered sensor with super-hydrophobic nanostructure surfaces for synchronous detection and electricity generation.* Nano Energy, 2017. **33**: p. 288-292.
23. She, H., et al., *One-step hydrothermal deposition of F:FeOOH onto BiVO4 photoanode for enhanced water oxidation.* Chemical Engineering Journal, 2020. **392**: p. 123703.
24. Ozay, H., P. Ilgin, and O. Ozay, *Hydrogen production via copper nanocatalysts stabilized by cyclen derivative hydrogel networks from the hydrolysis of ammonia borane and ethylenediamine bisborane.* International Journal of Hydrogen Energy, 2020. **45**(35): p. 17613-17624.
25. Grabi, H., et al., *Experimental and theoretical approach for the adsorption of ibuprofen in aqueous solution by biochars: application of conventional isotherms, statistical physics, and DFT.* Journal of Molecular Liquids, 2025. **438**: p. 128850.
26. Islam, M.R., et al., *Adsorption of Ibuprofen from Water Using Banana Peel Biochar: Experimental Investigation and Machine Learning Algorithms.* Water, 2024. **16**(23): p. 3469.
27. Siepmann, J. and N.A. Peppas, *Higuchi equation: Derivation, applications, use and misuse.* International Journal of Pharmaceutics, 2011. **418**(1): p. 6-12.
28. Foo, K.Y. and B.H. Hameed, *Insights into the modeling of adsorption isotherm systems.* Chemical Engineering Journal, 2010. **156**(1): p. 2-10.
29. Langmuir, I., *The adsorption of gases on plane surfaces of glass, mica and platinum.* Journal of the American Chemical society, 1918. **40**(9): p. 1361-1403.
30. Ho, Y.S. and G. McKay, *Pseudo-second order model for sorption processes.* Process Biochemistry, 1999. **34**(5): p. 451-465.